Comparative Study and Multi-Objective Optimization of Various Configurations in Natural Gas Liquefaction Process

Ahmadi, Samira; Jafari Nasr, Mohammad Reza*+

Department of Petroleum and Chemical Engineering, Science and Research Branch, Islamic Azad University, Tehran, I.R. IRAN

ABSTRACT: *PRICO process is a promising method for liquefaction of the natural gas which is sometimes used with some optional equipment. Although the PRICO process is widely used in natural gas liquefaction, the configuration leading to the most desirable performance has not been determined. The liquefaction rate and the energy consumption are two important factors to evaluate the performance of the PRICO process. In this study, the PRICO process with five different configurations was simulated and compared. By the means of the multi-objective optimization method, the liquefaction rate and the energy consumption were optimized, simultaneously, for each of the procedures. The five different simulated configurations are simple PRICO process, simple process with the third compressor, simple process with second heat exchanger, simple process with pre-cooling heat exchanger and full-set process. The optimization results demonstrated that the three-compressor and the full-set processes achieved the maximum liquefaction rate (96.51) and the minimum energy consumption (1219.53 kW), respectively. The economic analysis has also presented and revealed that the three-compressor process had the highest net profit (730.9288 M$/25 years) among the configurations. In other words, the three-compressor process outperformed other configurations with respect to the operation and economics (maximum liquefaction rate of 96.51 and net profit of 730.9288 M$/25 years).*

KEYWORDS: *PRICO Process; Liquefaction; NSGA-II; Genetic algorithm; Economic analysis.*

INTRODUCTION

Natural gas (NG) is one of the cleanest fossil fuels that has received lots of attention during the past decades [1]. There are two primary means of gas transportation: (1) pipeline, and (2) Liquefied Natural Gas (LNG) technology. Pipelines are highly expensive to construct, and there are cases where their construction is not economically viable, highlighting the need for taking advantage of natural gas liquefaction technology in which the LNG can be shipped to different destinations on vessels or cryogenic tanks [2]. Natural gas is usually composed of heavy compounds such as ethane, LPG, and gasoline which are important feed for petrochemical units [3, 4]. Separating Natural Gas Liquids (NGL) from gas reduces the cost of liquefaction [5]. Numerous research works have been reported on the NGL

** To whom correspondence should be addressed.*
+ E-mail: drnasr50@yahoo.ca
1021-9986/2021/6/1985-1998 14/$/6.04

recovery plant, most of which have focused on process optimization. *Ghorbani et al.* [3] optimized the refrigeration cycle in NGL recovery plant and reduced the energy consumption to 170 kW. Ghorbani and Roshani [4] applied advanced exergy and exert economic analysis of simultaneous production of NGL recovery and liquefaction and demonstrated that the priority was to improve the performance of the first multi-stream heat exchanger and the first and third compressors of the process. Liquefaction of natural gas, which cooled down the NG to liquefaction at -162℃ and decreased the gas volume to one six hundredths (1/600) and resulting in facilitating the transportation, is one of the most important cooling processes engaged in the gas industry [6-8]. Cascade, mixed-refrigerant, and expansion processes are the three primary models, based on which the conventional natural gas liquefaction processes are designed [9-12]. The liquefaction process of natural gas with single-mixed refrigerant (PRICO) has been widely used in small- and mid-scale LNG processes and peak shaving because of its simplicity, compactness, and low investment requirements. A mixed refrigerant refers to a blend of nitrogen and hydrocarbons (C1-C5) due to similarities between the refrigerant and the natural gas compositions which results in evaporating in the same range [13]. Due to the thermodynamic complexity of the NG liquefaction processes and the nonlinear relationships among the variables contributing to the process and the association of the variables with the objective functions, meta-heuristic methods are usually used to optimize such processes.

Numerous research works have been reported on the single-mixed refrigerant process, most of which have focused on the simulation and optimization of the process. *Mokarizadeh* and *Mowla* [14] simulated the simple NG liquefaction process with water coolers using the Aspen Hysys software, and the energy consumption of the process was optimized with a Genetic Algorithm (GA). *Xu et al.* [15] optimized the energy of PRICO process with a genetic algorithm and investigated the pinch point deeply. *Aspelund et al.* [16] optimized the one-compressor PRICO process through two methodologies, Tabu Search (TS) and Nelder-Mead Downhill Simplex (NMDS) search, and reduced the energy consumption by 23–36%. *Wahl et al.* [17] optimized the process that was previously simulated by *Aspelund* [15] using the SQP method. *Na et al.* [18] used a modified DIRECT (DIviding a hyper-RECTangle) algorithm with a sub-dividing step for considering hidden constraints to optimize the SMR process with three compressors and two heat exchangers. They ended up reducing their energy consumption by 18.9%. *Aslambakhsh et al.* [19] simulated PRICO process with two heat exchangers in the Aspen Hysys and optimized the net profit during the life-time of the process using GA. *Pham et al.* [20] could cut the energy consumption of the SMR process with four compressors by 30.6% by adding heavy components. *Qyyum et al.* [21] used a hydraulic turbine instead of the Joule–Thompson (JT) valve in a four-compressor SMR process and succeeded to save 16.5% of the energy consumption.

Several studies have investigated different objective functions to find the best functions [22, 23]. *Hatcher et al.* [22] optimized the C3/MCR process using 8 different objective functions to find the best objective function for the NG liquefaction process. They showed that the energy consumption and the sum of energy consumption and UA of the heat exchanger were the best objective functions. *Ghorbani et al.* [24] optimized the propane mixed refrigerant process based on a pinch, exergy analysis, and exert economic analysis. The unit cost of exergy and exergy efficiency were considered objective functions for multi-objective optimization of the process. Results showed a significant improvement with respect to economics and energetic features.

Song et al. [25] considered two objective functions for optimizing a single nitrogen expansion with carbon dioxide precooling: energy consumption and liquefaction rate and net profit were calculated. *Khan et al.* [26] undertook bi-objective optimization of UA and Specific Power Consumption (SPC) in the DMR process using the NSGA-II, with the results compared to those of the single-objective optimization using GA. Finally, they could reduce both SPC and UA by 24% and 3%, respectively. Various studies have also investigated the effect of ambient temperature on the process performance [13, 27]. Some studies have investigated a cycle using the cold energy of LNG [28-31].

According to the previous work, PRICO process was represented with some optional equipment which led to different configurations. It is noteworthy that the configuration leading to the most desirable performance has not been determined. In this study, PRICO process was investigated to define its best configuration by adding optional equipment items such as compressor, heat exchanger, and precooling heat exchanger, individually or simultaneously to consider all configurations. Mass flow rates of the refrigerant compounds, refrigerant pressures at the compressor outlet, throttle valve outlet in the cooling cycle, and the refrigerant temperature at the heat exchanger outlet were taken as optimization design variables. It should be noted that by using multi-objective optimization, the liquefaction rate and energy consumption were optimized simultaneously, which are the important factors to investigate natural gas liquefaction processes. Finally, in order to achieve a comprehensive comparison of configurations, economic analysis was performed and costs and net profits of configurations were reported and compared.

THEORETICAL SECTION

Case study

The present study investigates all available configurations of PRICO process. The considered configurations are illustrated in Fig. 1.

Mass flowrate, compositions, temperature, and pressure of the input NG flow are all assumed to be constant. Moreover, the ambient temperature and the temperature of the output refrigerant flow from the air coolers are assumed to be constant at 30℃ and 40℃, respectively. All constant process parameters are tabulated in Table 1.

Methods

Herein, the different configurations of the PRICO process are simulated in Aspen Hysys V.10. Peng-Robinson's Equation of State (EOS) is used to calculate the phase equilibrium. As mentioned earlier, due to the thermodynamic complexity and nonlinearity of the operating variables, powerful tools such as NSGA-II are commonly used for optimization purposes. Further explanation of the procedure of this algorithm can be found in the respective references [32, 33].

Process description

As shown in Fig. 1, in the heat exchanger, heat is taken from the gas (the NG flow) and the high-pressure refrigerant flows (the one leaving the last compressor) by means of the low-pressure refrigerant flow (the one leaving the pressure throttle valve) to provide the necessary refrigeration for liquefying the NG and the high-pressure refrigerant. In the cooling cycle, compressors and air coolers are used to increase the refrigerant pressure and lower the refrigerant temperature, respectively. Subsequently, the refrigerant is entered into the heat exchanger as a hot flow (flow 9 in Figure 1.a), where it loses its heat and becomes liquid (flow 10 in Figure 1.a). After passing through the throttle valve, the refrigerant enters the heat exchanger where it receives heat from two other flows and gets its temperature risen. Moreover, the NG in the heat exchanger gets cooled down and then liquefied.

Definition of the optimization problem

The multi-objective optimization is handled using NSGA-II. The objective functions of the problem are as follows:

$$\text{Minimize}\, f_1(x) = (\dot{m}_{LNG}/\dot{m}_{NG})^{-1} \quad (1)$$

$$\text{Minimize}\, f_2(x) = \sum_{k=1}^{n} W_{CMk} \quad (2)$$

Where, $(\dot{m}_{LNG}/\dot{m}_{NG})$, $\sum_{k=1}^{n} W_{CMk}$, $\dot{m}_{LNG}$ and $\dot{m}_{NG}$ are the liquefaction rate, process energy consumption (kW), flow rates of liquefied natural gas (kg/h), and natural gas (kg/h), respectively. Since the optimization is performed for five different configurations, the design variables of different configurations are different from one another. The mass flow rate of the refrigerant compounds, first heat exchanger output temperature, first and second compressor, and throttle valve output pressures comprised a total of nine common design variables between the five configurations. The third compressor output pressure, the second heat exchanger output temperature, and the pre-cooling heat exchanger output NG temperature are further added to the design variables of the PRICO process with three compressors, with two-heat exchangers, and with pre-cooling heat exchanger, respectively. All of the mentioned variables are included in the full-set process. Table 2 reports the upper and lower bounds of the design variables in different configurations [13].

In order to keep the process safe, it is necessary to respect some constraints. These constraints must be also applied in the optimization process:

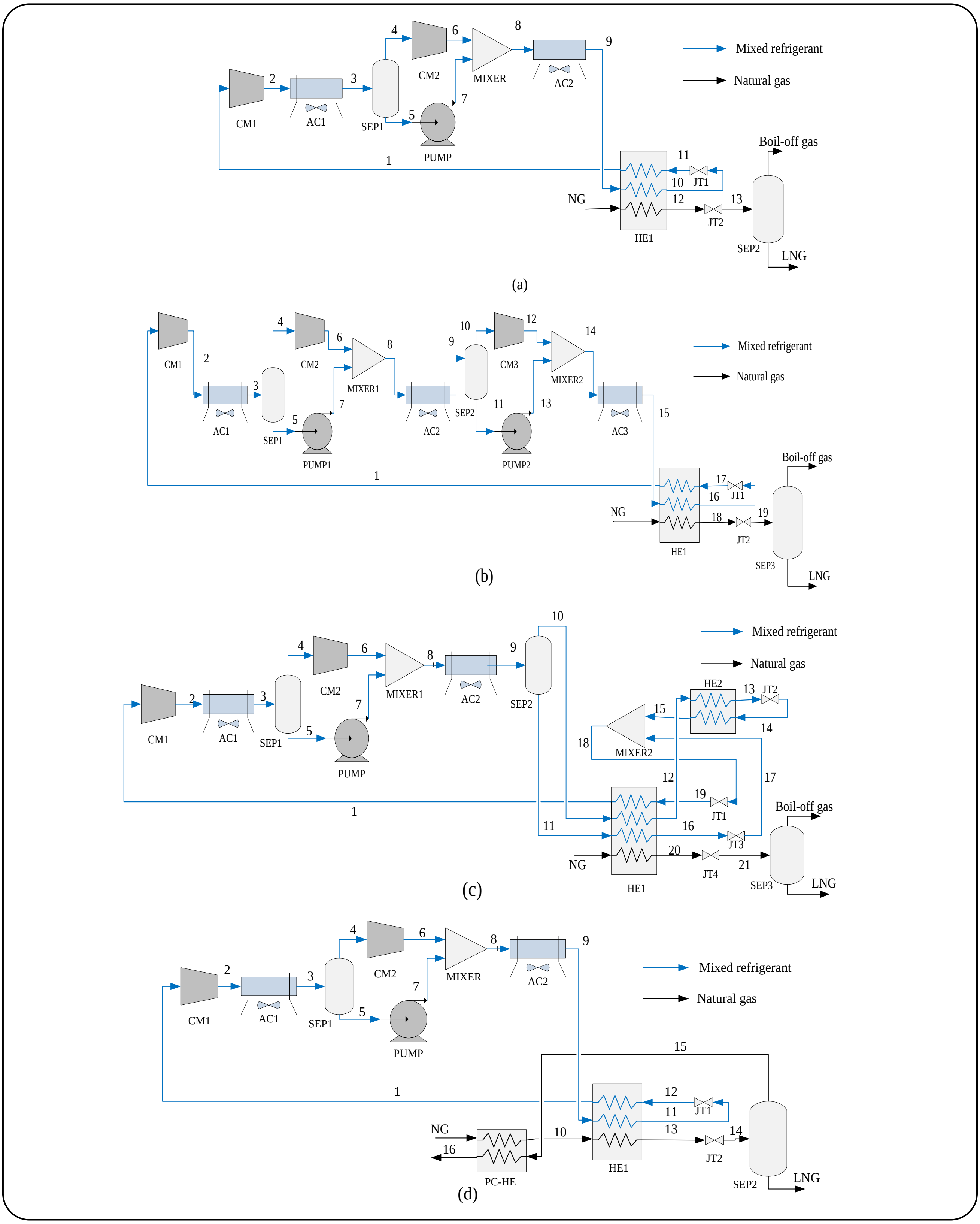

Fig. 1: The process flow diagram of a) the simple process, b) the three-compressor process, c) the two-heat exchanger process, d) the pre-cooling heat exchanger process and e) the full-set process.

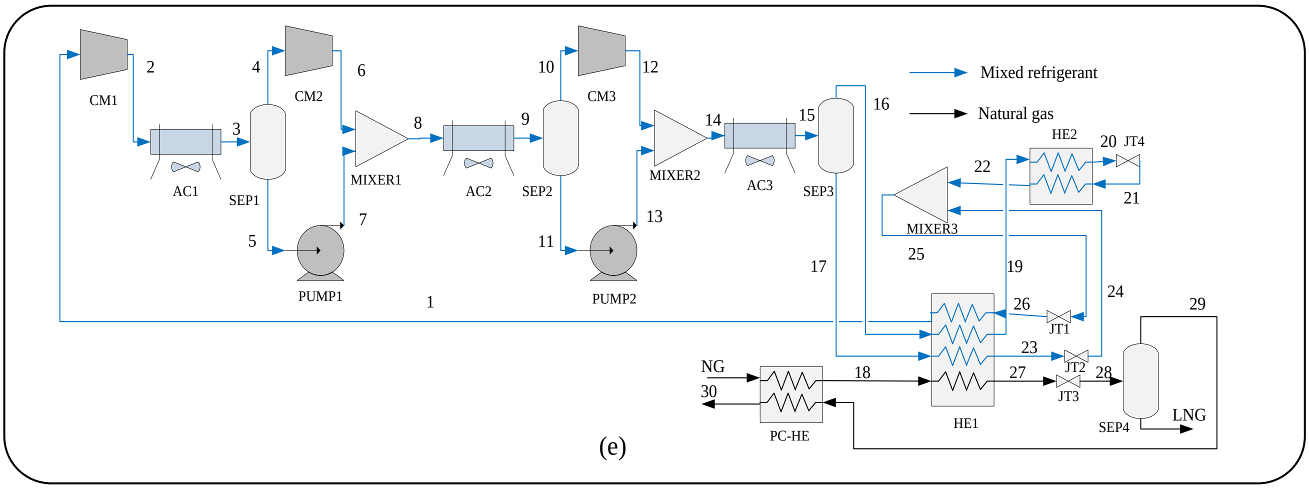

Fig. 1: The process flow diagram of a) the simple process, b) the three-compressor process, c) the two-heat exchanger process, d) the pre-cooling heat exchanger process and e) the full-set process.

Table 1: Process constant parameters.

Parameters	Value
Adiabatic compressor efficiency	78%
Minimum temperature approach of cold box (°C)	3
Pressure drop in cold box (bar)	0.5
Heat leakage of cold box	0%
Pressure drop in air coolers (bar)	0.5
Outlet temperature of air coolers (°C)	40
Natural gas	
Temperature (°C)	40
Pressure (bar)	50
Mass flow of feed gas (kgmol/h)	197
Molar composition (%)	
Methane	87.5
Ethane	5.5
Propane	2.1
i-Butane	0.3
n-Butane	0.5
i-Pentane	0.1
Nitrogen	4

Table 2: Upper and lower bounds of the design variables in different configurations.

Parameters	Simple process	Three-compressor process	Two-heat exchanger process	PC-heat exchanger process	Full-set process
Flow rate of MR (kg/h)					
$\dot{m}_{CH_4}$	50_120	50_120	50_120	50_120	50_120
$\dot{m}_{C_2H_6}$	80_300	80_300	80_300	80_300	80_300
$\dot{m}_{C_3H_8}$	30_150	30_150	30_150	30_150	30_150
$\dot{m}_{i-C_5H_{12}}$	30_150	30_150	30_150	30_150	30_150
$\dot{m}_{N_2}$	30_150	30_150	30_150	30_150	30_150
Pressure (kPa)					
P_{CM_1}	500_1500	500_1500	500_1500	500_1500	500_1500
P_{CM_2}	4000_7000	1500_4000	4000_7000	4000_7000	1500_4000
P_{CM_3}	---	4000_7000	---	---	4000_7000
P_{JT_1}	200_500	200_500	200_500	200_500	200_500
Temperature (°C)					
T_{HE_1}	-170_-150	-170_-150	-170_-150	-170_-150	-170_-150
T_{HE_2}	---	---	-175_-165	---	-175_-165
T_{PC-HE}	---	---	---	25_40	25_40

Table 3. The constraints for optimization of all configurations.

Constraints	Configurations
Heat exchanger	
$\Delta T_{\min}^{HE_1} \geq 3$	all configurations
$\Delta T_{\min}^{HE_2} \geq 3$	two-heat exchanger and full-set processes
$\Delta T_{\min}^{PC-HE} \geq 3$	PC-heat exchanger and full-set processes
Compressor	
$T_{suction}^{CM_1} > T_{suction,DewPoint}^{CM_1}$	all configurations
$T_{suction}^{CM_2} > T_{suction,DewPoint}^{CM_2}$	all configurations
$T_{suction}^{CM_3} > T_{suction,DewPoint}^{CM_3}$	Three-compressor and full-set processes

1) Minimum temperature approach of the heat exchanger must exceed 3°C.

2) Compressor input temperature must remain above its dew point to avoid entering any liquid into the compressor.

Constraints for all configurations are tabulated in Table 3.

As mentioned earlier, the energy consumption and liquefaction rate are simultaneously optimized with the help of NSGA-II, which is implemented by coupling the MATLAB software with Aspen Hysys. The optimization results are presented in the form of Pareto optimal fronts for different configurations. Further explanation of the procedure of this algorithm can be found in the respective references [34, 35]. The flowchart of the NSGA-II optimization is illustrated in Fig. 2.

Energy and exergy analysis

When evaluating the energy, the focus is on the energy consumption of the process. Accordingly, the lower the energy

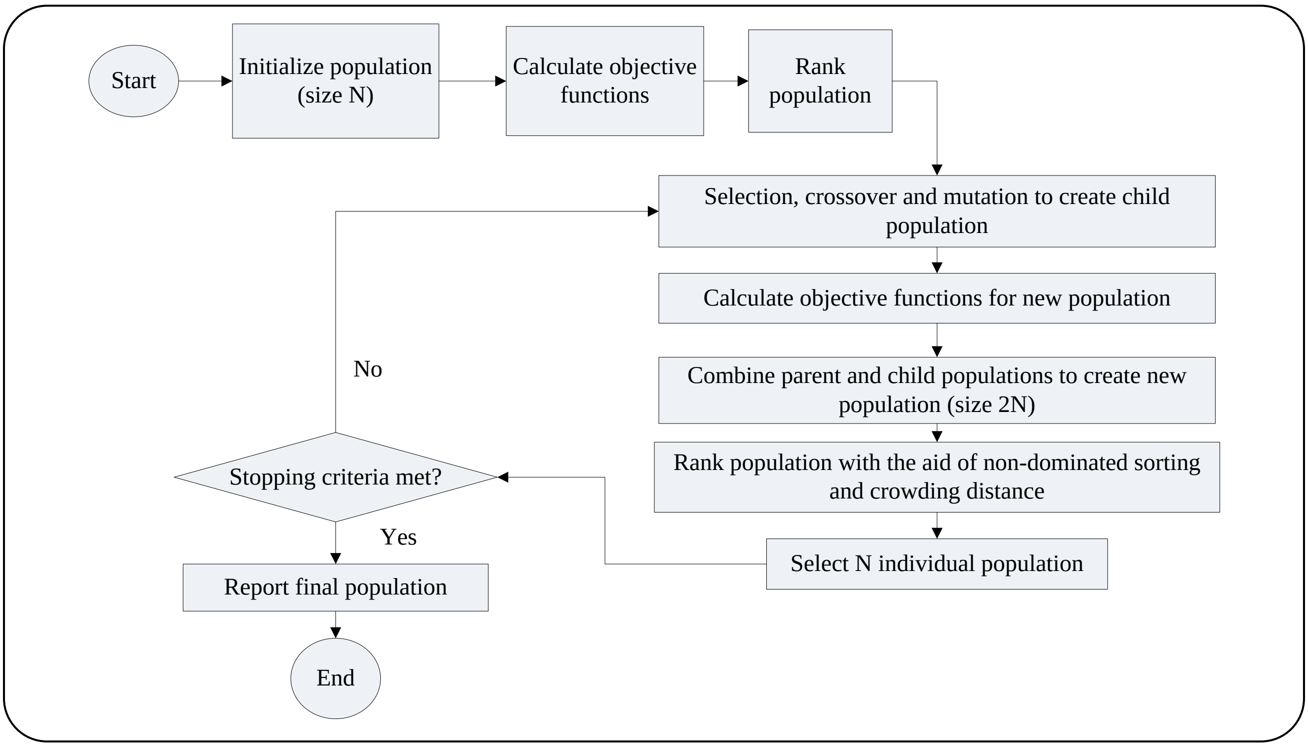

Fig. 2: Flowchart of the NSGA-II optimization.

consumption of the compressors, the more desirable would be the energy indices. Coefficient of Performance (COP) is the ratio of total heat taken from the cool source to the total work performed in the course of the cooling cycle. The higher the value of COP, the simpler is the heat absorption from the gas and the more energy-efficient in the process. Specific Power Consumption (SPC) refers to the total work performed in the course of the cooling cycle per kg of LNG. The lower the SPC, the lower the energy consumption for producing LNG. The exergy efficiency is calculated by the exergies of the fuel and product.

Economic analysis

The optimized processes will economically analyze and compare their results. In this section, the investment and operating costs, LNG sales costs, the payback period, and the net profit are considered. Moreover, the cost of primary equipment items including the heat exchangers and compressors are taken into account as the investment cost of the process. Next, in order to calculate the accurate value of the investment cost including the set-up, piping, and completion costs, the costs of compressors and heat exchangers are multiplied by 2.5 and 3.5, respectively [34]. The respective equations are as follows [19, 36]:

$$C_{CM}(\$) = 580000 + 20000 \times W^{0.6} \tag{3}$$

$$C_{MSHE}(\$) = 425 \times A \tag{4}$$

where, C_{CM}, W, $C_{MSHE,}$ and A are purchased cost of a compressor ($), energy consumption (kW), purchased cost of a heat exchanger ($), and heat transfer surface (m²), respectively. In these equations, the purchased costs of a heat exchanger and compressor are presented in 2011 and 2010, respectively. To obtain the costs in 2018, Chemical Engineering’s Plant Cost Index (CEPCI) is utilized [37]. The operating cost is mainly composed of the cost of energy consumed by the compressors. The operating cost is herein calculated through the following equation [19]:

$$OPEX(\$/25\,years) = W \times 24 \times 330 \times \sum_{i=1}^{25} n_i \tag{5}$$

where, OPEX, W and $\sum_{i=1}^{25} n_i$ are the 25-year operating cost ($/25 years), the total energy consumption (kW) of the compressors, and the total unit cost of energy for the entire 25-years lifetime of the plant (c/ kWh 25 years), respectively. In this equation, the number of working days per year and the lifetime of the plant are set to 330 days

Table 4: Comparison of present simulation outputs with that of the previous work.

Parameters	Previous work[13]	Present work	Error percent(%)
Adiabatic compressor efficiency	78%	78%	---
Outlet temperature of coolers (°C)	20	20	---
Mass flow of feed gas (kg/s)	1	1	---
COP	0.762	0.760	0.262
Energy consumption (kW)	1013.5	1014.23	0.072

and 25 years, respectively. The unit cost of energy in 2018 (n_1) has been 6.91 c/kWh [38].

The profit obtained from this process is the sales amount of LNG which is computed through the following equation [19]:

$$\text{Sale of LNG } (\$/25\text{years}) = (q^{ST} \times 330) \times \sum_{i=1}^{25} L_i \quad (6)$$

In which, q^{ST} and $\sum_{i=1}^{25} L_i$ are the liquefied natural gas volume per day (ft^3 / day), total unit profit of the LNG sale for the entire 25-year life of the plant (\$/ 1000 ft^3 25 years), respectively. The unit profit of LNG in 2018 (L_1) has been 4.92 $\$/1000\ ft^3$ [39]. Net profit for this process is [19]:

$$\text{Net profit} (\$/25 \text{ years}) = \text{profit from sale of LNG} - \text{total cost} \quad (7)$$

In which, total cost includes both capital (\$) and operating costs (\$ / 25 years) which were discussed earlier.

RESULTS AND DISCUSSION

In this research, five different configurations of PRICO process are simulated, optimized, and then compared. Multi-objective optimization is undertaken to maximize the liquefaction rate and minimize the energy consumption simultaneously. In order to attain a comprehensive comparison of configurations, costs, payback periods, and net profits of configurations are reported and compared. Finally, one process is selected as the best configuration with respect to the operation and economy.

Simulation verification

In order to verify the simulation results, the outcomes of the methodology presented in this work are compared to those of work by *Xu et al.* [13] in which a PRICO process was modeled in the Aspen Hysys. The input data and the results of the present study and previous research are tabulated in Table 4. The results indicate an acceptable accuracy of the simulations performed in the present work. Relative errors for the energy consumption and COP are as low as 0.07% and 0.26%, respectively.

Optimization results

In this research, NSGA-II was used to optimize objective functions simultaneously. Optimal results of different configurations are obtained in the form of Pareto optimal fronts. The Pareto optimal front of the simple PRICO process is clarified in Fig. 3. In this plot, the vertical and horizontal axes correspond to the objective functions, the liquefaction rate, and energy consumption, respectively. As seen from the Figure, the objective functions had a conflict with each other which indicates that these are appropriate functions for multi-objective optimization. Since the problem targeted the maximization of the liquefaction rate at the minimum energy consumption, the Pareto optimal front that was closer to the horizontal axis was associated with a higher liquefaction rate, while the one that was closer to the vertical axis resulted in lower energy consumption. As it is demonstrated in Figure 3, three different designs have been identified on the plot: (A) the design with the lowest energy consumption, (B) the final optimal design (closest distance to the ideal point), and (C) the design leading to maximum liquefaction rate. The ideal point refers to a virtual point at which all objective functions exhibit their best values. For more information about finding the final optimal design, the respective references [40, 41] can be addressed.

In order to attain a comprehensive comparison of optimization results, the Pareto optimal fronts of configurations are demonstrated in Fig. 4. According to Fig. 4, considering the energy consumption (under equal

Table 5: Design parameters of final optimal designs for each configuration.

Parameters	Simple process	Three-compressor process	Two-heat exchanger process	PC-heat exchanger process	Full-set process
Flow rate of MR (kg/h)					
$\dot{m}_{CH_4}$	100.78	100.3	87.96	97.66	103.69
$\dot{m}_{C_2H_6}$	187.55	184.45	170.71	157.81	188.78
$\dot{m}_{C_3H_8}$	77.28	67.45	77.37	77.40	75.55
$\dot{m}_{i-C_5H_{12}}$	102.72	100.73	90.81	95.10	89.10•
$\dot{m}_{N_2}$	107.27	107.83	97.78	93.76	93.42
Pressure (kPa)					
P_{CM_1}	1202.54	1098.19	1358.42	1233.93	1186.37
P_{CM_2}	4448.48	2408.94	5278.12	5226.38	2193.24
P_{CM_3}	---	5555.65	---	---	۵۲۴۶,۳۳
P_{JT_1}	444.60	425.47	337.88	364.99	459.11
Temperature (°C)					
T_{HE_1}	-163	-167.8	-163.61	---	-159
T_{HE_2}	---	---	-168	-164	-169
T_{HE-PC}	---	---	---	37.01	36.33

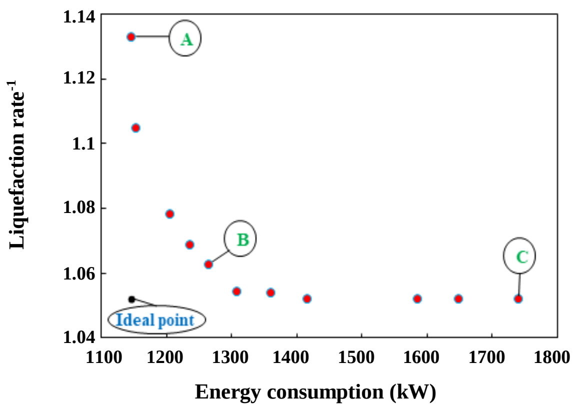

Fig. 3: Pareto optimal front of the simple process.

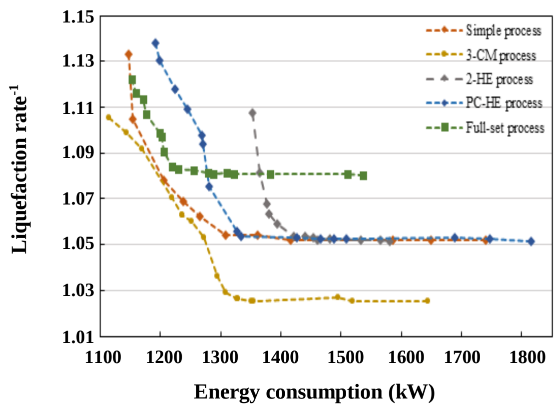

Fig. 4: Pareto optimal fronts of all configurations.

liquefaction rate), the three-compressor process provided the most optimal performance, while the two-heat exchanger process was found to lead to the maximum energy consumption, and considering the liquefaction rate (under equal energy consumption), the three-compressor process provided the highest liquefaction rate, while the full-set, pre-cooling heat exchanger and two-heat exchanger processes resulted in a minimum liquefaction rate in various ranges of energy consumption. In other words, the Pareto optimal fronts of the three-compressor process and full-set process were the closest and the furthest ones to the horizontal and vertical axes, hence the best and the worst configurations were three-compressor and full-set processes, respectively.

Details of all final optimal designs (closest distance to the ideal point) for different configurations are presented in Table 5.

Fig. 5 presents the energy consumption of final optimal designs in different configurations. According to this Figure, the final optimal design for the full-set and two-heat

Table 6: Objective functions, energy and exergy efficiencies of final optimal designs in all configurations.

	Simple process	Three-compressor process	Two-heat exchanger process	PC heat exchanger process	Full-set process
Energy consumption (kW)	1264.55	1295.21	1294.08	1326.89	1219.53
Liquefaction rate	94.1	96.51	94.41	94.7	92.23
SPC (kJ/kg LNG)	0.37	0.37	0.41	0.38	0.36
COP	0.65	0.651	0.59	0.62	0.66
Exergy Efficiency (%)	47.81	53.34	51.1	50.65	52.66

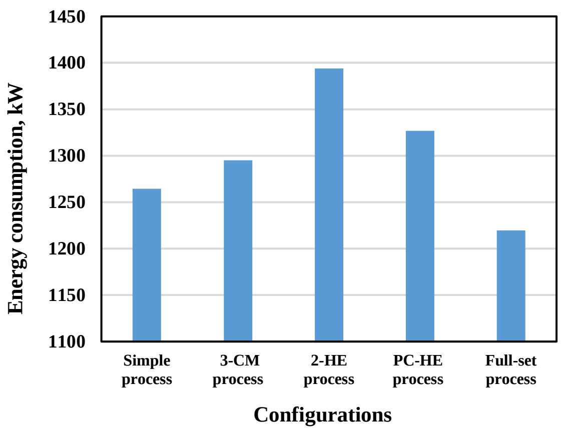

Fig. 5: Energy consumption of final optimal designs in configurations.

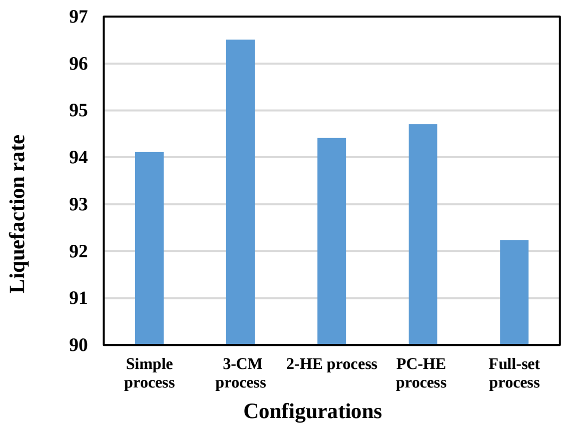

Fig. 6: Liquefaction rate of final optimal designs in configurations.

exchanger process led to the best (1219.53 kW) and the worst energy consumptions (1394.08 kW), respectively. This figure also indicates that adding all optional equipment items to the simple process individually and simultaneously led to the worsening and improvement of the energy consumption, respectively. In addition, exact numerical values of energy consumption for optimal designs in different configurations are displayed in Table 6.

Figure 6 presents the liquefaction rate of NG for final optimal designs in different configurations. This Figure implies that the final optimal design for the three-compressor and the full-set process provided the best (96.51) and the worst liquefaction rates (92.23), respectively. This figure also illustrates that adding all optional equipment items to the simple process individually and simultaneously led to the improvement and worsening of the liquefaction rate, respectively. In addition, exact numerical values of the liquefaction rate for the optimal designs in different configurations are given in Table 6.

The values of objective functions, SPC, COP, and exergy efficiency of final optimal designs in different configurations are demonstrated in Table 6. As demonstrated in Figs. 5 and 6, the most optimal performance in terms of energy consumption and liquefaction rate are the full-set (1219.53 kW) and three-compressor (96.51) processes, respectively. Table 6 points out that the full-set process reached the most desirable value of SPC (0.36 kJ/kg LNG) and COP (0.66) due to its lowest energy consumption. According to Table 6, the three-compressor process achieved the best exergy efficiency (53.34%) among all configurations.

Economic analysis

The values of CAPEX, OPEX, payback period and net profit of final optimal designs in different configurations are demonstrated in Table 7. According to Table 7, the precooling heat exchanger and full-set processes had the lowest (13.4391 M$) and highest (16.8918 M$) capital costs, respectively. Adding all optional equipment items to the simple process, in order to assemble the full-set process, increased the CAPEX significantly. Meanwhile, due to the fact that the full-set process consumes less energy than other configurations, its operating cost would be less

Table 7: CAPEX, OPEX, payback period and net profit of final optimal designs in configurations.

	Simple process	Three-compressor process	Two-heat exchanger process	PC heat exchanger process	Full-set process
CAPEX (M$)	14.3854	16.2532	13.7522	13.4391	16.8918
OPEX (M$/25 years)	25.2319	25.8436	27.8163	26.4757	24.3334
Payback period (year)	2.67	2.95	2.58	2.5	3.2
Net profit (M$/25years)	683.3178	730.9288	716.0953	۷۱۹,۹۶۵۲	۶۹۹,۳۸۰۴

Table 8: The best optimal values of objective functions and criteria among configurations.

The best optimal value of	Simple process	Three-compressor process	Two-heat exchanger process	PC heat exchanger process	Full-set process
energy consumption					√
liquefaction rate		√			
energy indices					√
exergy efficiency		√			
Net profit		√			

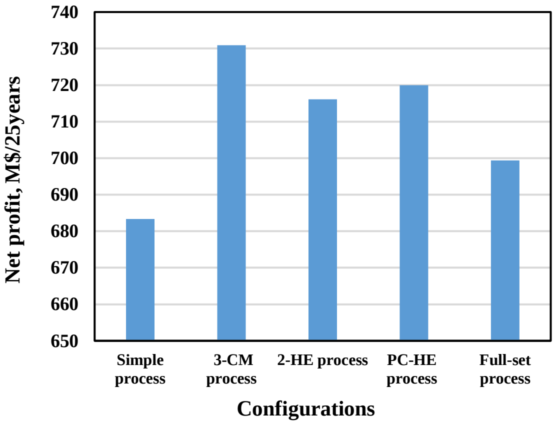

Fig. 7: Net profit of final optimal designs in configurations.

than the others (24.3334 M$/25 years). By definition, the payback period is the ratio of the equipment cost to the annual net profit. So, it is clear that the longest payback period is attributed to the full-set process (3.2 years). Net profit of all configurations as an economic criterion is reported in Table 7. As can be found in Table 7, the three-compressor process is associated with the highest net profit (730.9288 M$/25years), making it economically the best design.

Also, Fig. 7 illustrates the values of net profit of final optimal designs in all configurations. Adding the third compressor to the simple process significantly increased the net profit (7% more than the simple process). Adding the optional equipment to the simple process individually imposed an insignificant additional cost to the simple process, on the other hand, significantly improved the liquefaction rate over the simple process, and thereby raised the net profit.

In terms of technical evaluation of different configurations, the objective functions were considered for the optimization, and the liquefaction rate and energy consumption were taken as the comparison criteria. Considering the liquefaction rate, the three-compressor process outperformed the other configurations, while the full-set process outperformed with respect to energy consumption. In order to choose a single configuration as the best design based on the comparisons performed in this research, the net profits of the full-set and three-compressor processes were compared. The data provided that the three-compressor process achieves 4.51% higher net profit than the full-set process. Therefore, from the designer's point of view, the three-compressor process can be referred to as the desired configuration. The best optimal values of objective functions and criteria among the configurations are briefly illustrated in Table 8.

CONCLUSIONS

Herein, various configurations of the PRICO process were considered to determine the configuration of PRICO process which outperformed with respect to operation and economics. All configurations including simple process, simple process with third compressor, simple process with a second heat exchanger, a simple process with a pre-cooling heat exchanger, and full-set PRICO processes were optimized by NSGA-II. Mass flow rates of the refrigerant compounds, refrigerant pressures at the compressor outlet and throttle valve outlet in the cooling cycle, and the refrigerant temperature at the heat exchanger outlet were taken as optimization design variables. The maximum liquefaction rate and minimum energy consumption were reached simultaneously by multi-objective optimization. According to this study, the following conclusions were drawn:

1) Adding optional equipment individually to the simple PRICO process improved the liquefaction rate and worsened the energy consumption.

2) Adding optional equipment simultaneously to the simple PRICO process improved the energy consumption and worsened the liquefaction rate.

3) Three-compressor and full-set processes achieved the maximum liquefaction rate (96.51) and minimum energy consumption (1219.53 kW), respectively.

4) Net profit of the three-compressor and full-set processes were calculated to be 730.92 and 699.38 M$/25 years, respectively. In other words, considering both operation and economic points of view, the three-compressor process was introduced as the desired configuration.

Nomenclature

A	Heat transfer surface, m^2
C	Purchased cost, $
f	Objective function
L	LNG sale cost in a year, $ / 1000 ft^3
$\dot{m}$	Mass flow rate, kg/h
n	Energy consumption cost of a year, c/kWh
q^{ST}	Liquefied natural gas volume per day, ft^3/day
W	Energy consumption, kW

Subscripts

CM	Compressor
HE	Heat exchanger
PC HE	Precooling heat exchanger
i	i^{th} year
JT	Joule-Thompson valve
k	k_{th} compressor
MSHE	Multi-stream heat exchanger
SEP	Separator
min	minimum

Abbreviations

AC	Air cooler
CAPEX	Capital cost
COP	Coefficient of performance
C_3 / MCR	Propane pre-cooled mixed refrigerant process
DMR	Double mixed refrigerant process
GA	Genetic algorithm
M$	Million dollar
MR	Mixed refrigerant
NG	Natural gas
NSGA	Non-dominated sorting genetic algorithm
OPEX	Operating cost
PRICO	Poly refrigerant integral cycle operation
SMR	Single mixed refrigerant process
SPC	Specific power consumption, kJ/kg LNG

Received : March 16, 2020 ; Accepted : July 20, 2020

REFERENCES

[1] Sun W., Hu P., Chen Z., Jia L., Performance of Cryogenic Thermoelectric Generators in LNG Cold Energy Utilization, *Energy Conversion and Management*, **46**:789-796 (2006).

[2] Ghaebi H., Parikhani T., Rostamzadeh H., Energy, Exergy and Thermoeconomic Analysis of a Novel Combined Cooling and Power System Using Low-Temperature Heat Source and LNG Cold Energy Recovery, *Energy Conversion and Management*, **150**:678-692 (2017).

[3] Ghorbani B., Salehi G.R., Ghaemmaleki H., Amidpour M., Hamedi M.H., Simulation and Optimization of Refrigeration Cycle in NGL Recovery Plants with Exergy-Pinch Analysis, *Journal of Natural Gas Science and Engineering*, **7**:35-43 (2012).

[4] Ghorbani B., Roshani H., Advanced Exergy and Exergoeconomic Analysis of the Integrated Structure of Simultaneous Production of NGL Recovery and Liquefaction, *Transport Phenomena in Nano Micro Scales*, **6, Special Issue**:8-14 (2018).

[5] Ghorbani B., Hamedi M.H., Amidpour M., Development and Optimization of an Integrated Process Configuration for Natural Gas Liquefaction (LNG) and Natural Gas Liquids (NGL) Recovery with a Nitrogen Rejection Unit (NRU), *Journal of Natural Gas Science and Engineering*, **34**:590-603 (2016).

[6] Remeljej C.W., Hoadley A.F.A., An exergy Analysis of Small-Scale Liquefied Natural Gas (LNG) Liquefaction Process, *Energy*, **31**:2005-2019 (2006).

[7] Ali W., Qyyum M.A., Qadeer K., Lee M., Energy Optimization for Single Mixed Refrigerant Natural Gas Liquefaction Processes Using the Metaheuristic Vortex Search Algorithm, *Applied Thermal Engineering*, **25**:782-791 (2018).

[8] Shi X., Che D., A Combined Power Cycle Utilizing Low-Temperature Waste Heat and LNG Cold Energy, *Energy Conversion and Management*, **50**:567-575 (2009).

[9] Ghorbani B., Mehrpooya M., Hamedi M.H., Amidpour M., Exergoeconomic Analysis of Integrated Natural Gas Liquids (NGL) and Liquefied Natural Gas (LNG) Processes, *Applied Thermal Engineering*, **113**:1483-1495 (2017).

[10] Palizdar A., Ramezani T., Nargessi Z., AmirAfsharar S., Abbasi M., Vatani A., Thermodynamic Evaluation of Three Mini-Scale Nitrogen Single Expansion Processes for Liquefaction of Natural Gas Using Advanced Exergy Analysis, *Energy Conversion and Management*, **150**:637-650 (2017).

[11] Castillo L., Dahouk M.M., Scipio S.D., Dorao C.A., Conceptual Analysis of the Precooling Stage for LNG Processes, *Energy Conversion and Management*, **66**:41-47 (2013).

[12] Palizdar A., Ramezani T., Nargessi Z., Amirafshar S., Abbasi M., Vatani A., Advanced Exergoeconomic Evaluation of a Mini-Scale Nitrogen Dual Expander Process for Liquefaction of Natural Gas, *Energy*, **168**:542-557 (2019).

[13] Xu X., Liu J., Jiang C., Cao L., The Correlation Between Mixed Refrigerant Composition and Ambient Conditions in the PRICO LNG Process, *Applied Energy*, **102**:1127-1136 (2013).

[14] Mokarizadeh Haghighi Shirazi M., Mowla D., Energy Optimization for Liquefaction Process of Natural Gas in Peak Shaving Plant, *Energy*, **35**:2878-2885 (2010).

[15] Xu X., Liu J., Cao L., Optimization and Analysis of Mixed Refrigerant Composition for the PRICO Natural Gas Liquefaction Process, *Cryogenics*, **59**:60-69 (2014).

[16] Aspelund A., Gundersen T., Myklebust J., Nowak M.P., Tomasgard A., An Optimization-Simulation Model for a Simple LNG Process, *Computers and Chemical Engineering*, **34**:1606-1617 (2010).

[17] Wahl P.E., Lovseth S.W., Molnvik M.J., Optimization of a Simple LNG Process Using Sequential Quadratic Programming, *Computers and Chemical Engineering*, **56**:27-36 (2013).

[18] Na J., Lim Y., Han C., A Modified DIRECT Algorithm for Hidden Constraints in an LNG Process Optimization, *Energy*, **126**:488-500 (2017).

[19] Aslambakhsh A.H., Moosavian M.A., Amidpour M., Hosseini M., Amirafshar S., Global Cost Optimization of a Mini-Scale Liquefied Natural Gas Plant, *Energy*, **148**:1191-1200 (2018).

[20] Pham T.N., Long N.V.D., Lee S., Lee M., Enhancement of Single Mixed Refrigerant Natural Gas Liquefaction Process Through Process Knowledge Inspired Optimization and Modification, *Applied Thermal Engineering*, **110**: 1230-1239 (2017).

[21] Qyyum M.A., Ali W., Long N.V.D., Khan M.S., Lee M., Energy Efficiency Enhancement of a Single Mixed Refrigerant LNG Process Using a Novel Hydraulic Turbine, *Energy*, **144**:968-976 (2018).

[22] Hatcher P., Khalilpour R., Abbas A., Optimisation of LNG Mixed-Refrigerant Processes Considering Operation and Design Objectives, *Computers and Chemical Engineering*, **41**:123-133 (2012).

[23] Wang M., Khalilpour R., Abbas A., Thermodynamic and Economic Optimization of LNG Mixed Refrigerant Processes, *Energy Conversion and Management*, **88**:947-961 (2014).

[24] Ghorbani B., Hamedi M.H., Shirmohammadi R., Hamedi M., Mehrpooya M., Exergoeconomic Analysis and Multi-Objective Pareto Optimization of the C3MR Liquefaction Process, *Sustainable Energy Technologies and Assessments*, **17**:56-67 (2016).

[25] Song R., Cui M., Liu J., Single and Multiple Objective Optimization of a Natural Gas Liquefaction Process, *Energy*, **124**:19-28 (2017).

[26] Khan M.S., Karimi I.A., Lee M., Evolution and Optimization of the Dual Mixed Refrigerant Process of Natural Gas Liquefaction, *Applied Thermal Engineering*, **96**:320-329 (2016).

[27] Moein P., Sarmad M., Ebrahimi H., Zare M., Pakseresht S., Vakili S.Z., APCI- LNG Single Mixed Refrigerant Process for Natural Gas Liquefaction Cycle: Analysis and Optimization, *Journal of Natural Gas Science and Engineering*, **26**:470-479 (2015).

[28] Ahmadi M.H., Mehrpooya M., Pourfayaz F., Exergoeconomic Analysis and Multi-Objective Optimization of Performance of a Carbon Dioxide Power Cycle Driven by Geothermal Energy with Liquefied Natural Gas as its Heat Sink, *Energy Conversion and Management*, **119**:422-434 (2016).

[29] Ahmadi M.H., Mohammadi A., Pourfayaz F., Mehrpooya M., Bidi M., Valero A., Uson S., Thermodynamic Analysis and Optimization of a Waste Heat Recovery System for Proton Exchange Membrane Fuel Cell Using Transcritical Carbon Dioxide Cycle and Cold Energy of Liquefied Natural Gas, *Journal of Natural Gas Science and Engineering*, **34:**428-438 (2016).

[30] Ahmadi M.H., Mehrpooya M., Abbasi S., Mohammadi A., Pourfayaz F., Bruno J.C., Thermo-Economic Analysis and Multi-Objective Optimization of a Transcritical CO_2 Power Cycle Driven by Solar Energy and LNG Cold Recovery, *Thermal Science and Engineering Progress*, **4**:185-196 (2017).

[31] Ghorbani B., Mahyari K.B., Mehrpooya M., Hamedi M.H., Introducing a Hybrid Renewable Energy System for Production of Power and Fresh Water Using Parabolic Trough Solar Collectors and LNG Cold Energy Recovery, *Renewable Energy*, **148**:1227-1243 (2020).

[32] Maghsoudi P., Sadeghi S., Khanjarpanah H., Gorgani H.H., A comprehensive Thermo-Economic Analysis, Optimization and Ranking of Different Microturbine Plate-Fin Recuperators Designs Employing Similar and Dissimilar Fins on Hot and Cold Sides with NSGA-II Algorithm and DEA Model, *Applied Thermal Engineering*, **130**:1090-1104 (2018).

[33] Maghsoudi P., Sadeghi S., Gorgani H.H., Comparative Study and Multi-Objective Optimization of Plate-Fin Recuperators Applied in 200 kW Microturbines Based on Non-Dominated Sorting and Normalization Method Considering Recuperator Effectiveness, Exergy Efficiency and Total Cost, *International Journal of Thermal Sciences*, **124**:50-67 (2018).

[34] Maghsoudi P., Sadeghi S., Hanafizadeh P., Thermoeconomic Optimization and Comparison of Plate-Fin Heat Exchangers Using Louver, Offset Strip, Triangular and Rectangular Fins Applied in 200 kW Microturbines, *Journal of Heat Transfer*, **139(10)**: 101801 (2017).

[35] Maghsoudi P., Sadeghi S., Xiong Q., Aminossadati S.M., A Multi-Factor Methodology for Evaluation and Optimization of Plate-Fin Recuperators for Micro Gas Turbine Applications Considering Payback Period as Universal Objective Function, *International Journal of Numerical Methods for Heat & Fluid Flow*, **30(5)**: 2411-2438 (2019).

[36] Towler G., Sinnott R., Chemical Engineering Design: Principles, Practice and Economics of Plant and Process Design, 2nd ed, Capital cost estimating, *United Kingdom: Butterworth-Heinemann*, (2013).

[37] Chemical Engineering Essential for the CPI Professional, *Chemical Engineering Plant Cost Index*, https://www.chemengonline.com/2019-cepci-updates-january-prelim-and-december-2018-final/2018/ (accessed 10 September 2019).

[38] U.S. Energy Information Administration (eia), *Electric Power Monthly*, https://www.eia.gov/electricity/monthly/, December 2018 (Accessed 6 September 2019).

[39] U.S. Energy Information Administration (eia), *Price of Liquefied Natural Gas Exports*, https://www.eia.gov/dnav/ng/hist/n9133us3M.htm, October 2018 (Accessed 6 September 2019).

[40] Maghsoudi P., Sadeghi S., A Novel Economic Analysis and Multi-Objective Optimization of a 200-kW Recuperated Micro Gas Turbine Considering Cycle Thermal Efficiency and Discounted Payback Period, *Applied Thermal Engineering*, **166**:114644 (2020).

[41] Hanafizadeh P., Maghsoudi P., Exergy, Economy and Pressure Drop Analyses for Optimal Design of Recuperator Used in Microturbine, *Energy Equipment and Systems*, **5(2)**: 95-113 (2017).